

*Supplements of*

**First deployment of active AirCore in a volcanic plume at Mount Etna**

Johannes Degen et al.

**Table 1.** Technical details of individual components of the (active AirCore sampling and analysis) setup illustrated in Fig. 2.

label in Fig. 2	function	type or manufacturer	specification
AirCore	sample volume	Silconert® stainless steel	length 75 m, inner diameter 2.9 mm, volume 500 cm <sup>3</sup>
p	combined pressure & temperature sensor	AMSYS AMS 5915	one barometric, one absolute and two differential
T	temperature sensor	Innovative Sensor Technology	PT100
dryer	drying tube	Mg(ClO <sub>4</sub> ) <sub>2</sub> (and glass wool)	15 cm 1/4" polyvinylchloride tube
battery	powering	2x18650 Li-ION Keppower 3500mAh	7.4 V protected against undervoltage
LoRa	data transmission	Adafruit LoRa RFM95W	900 MHz
esp32	microcontroller	Adafruit HUZZAH32 ESP32 Feather Board	240 MHz dual core
rtc + sd	Real Time Clock & micro SD card storage	AdaLogger FeatherWing	
gps	positional data	Adafruit PA I010D	
oled	display	Adafruit FeatherWing	1.3" diagonal, 128 x 64 pixels
pump	sample collection	KNF NMP015	6 V, max. 1.6 l/min, lowest pressure 400 mbar abs.
orifice	critical orifice	Lenox laser Inc.	50 ± 10 μ m diameter, flow at STP: 21.5 sccm
CO <sub>2</sub>	Non-dispersive infrared CO <sub>2</sub> sensor	Senseair K30 FR	0—5000 ppm, operated in diffusive mode
CRDS	cavity ring down spectrometer	Picarro G2401	operated in inlet mode, precision 0.03 ppm (CO <sub>2</sub> ), 0.2 ppb (CH <sub>4</sub> ), 5 ppb (CO)
needle valve	CRDS flow regulation	Swagelok	SS-SS2 1/8" stainless steel

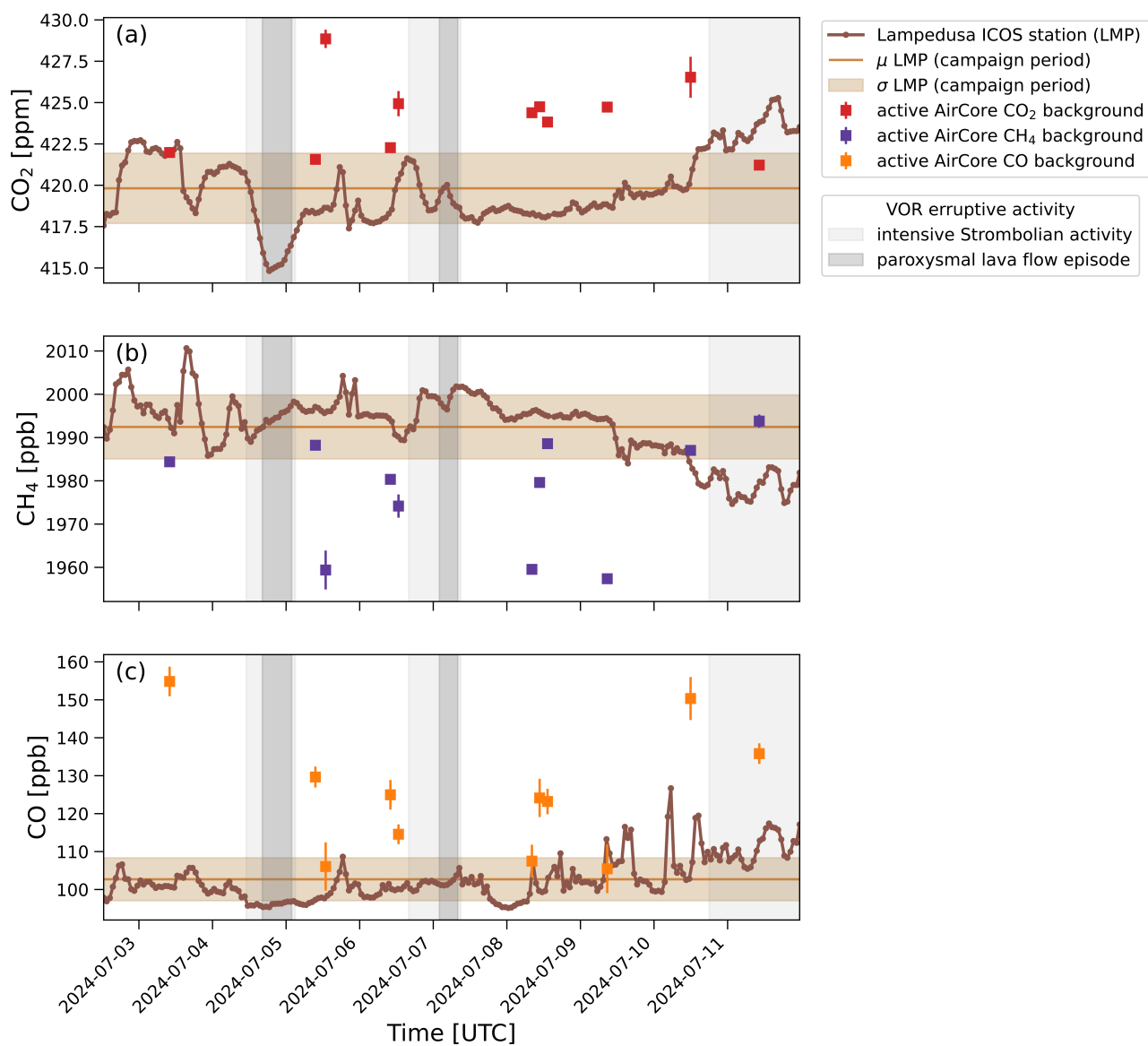


**Figure S1.** Overview of the local and regional background determination for the different species CO<sub>2</sub>, CH<sub>4</sub> and CO (panel a-c). Coloured symbols show flight individual local background values derived from active AirCore sampling during hovering phase of the UAV near the launch site. Measurement data from Lampedusa ICOS site (station code LMP) served as estimate for regional background values are shown with  $\mu$  and  $\sigma$  within the campaign period.

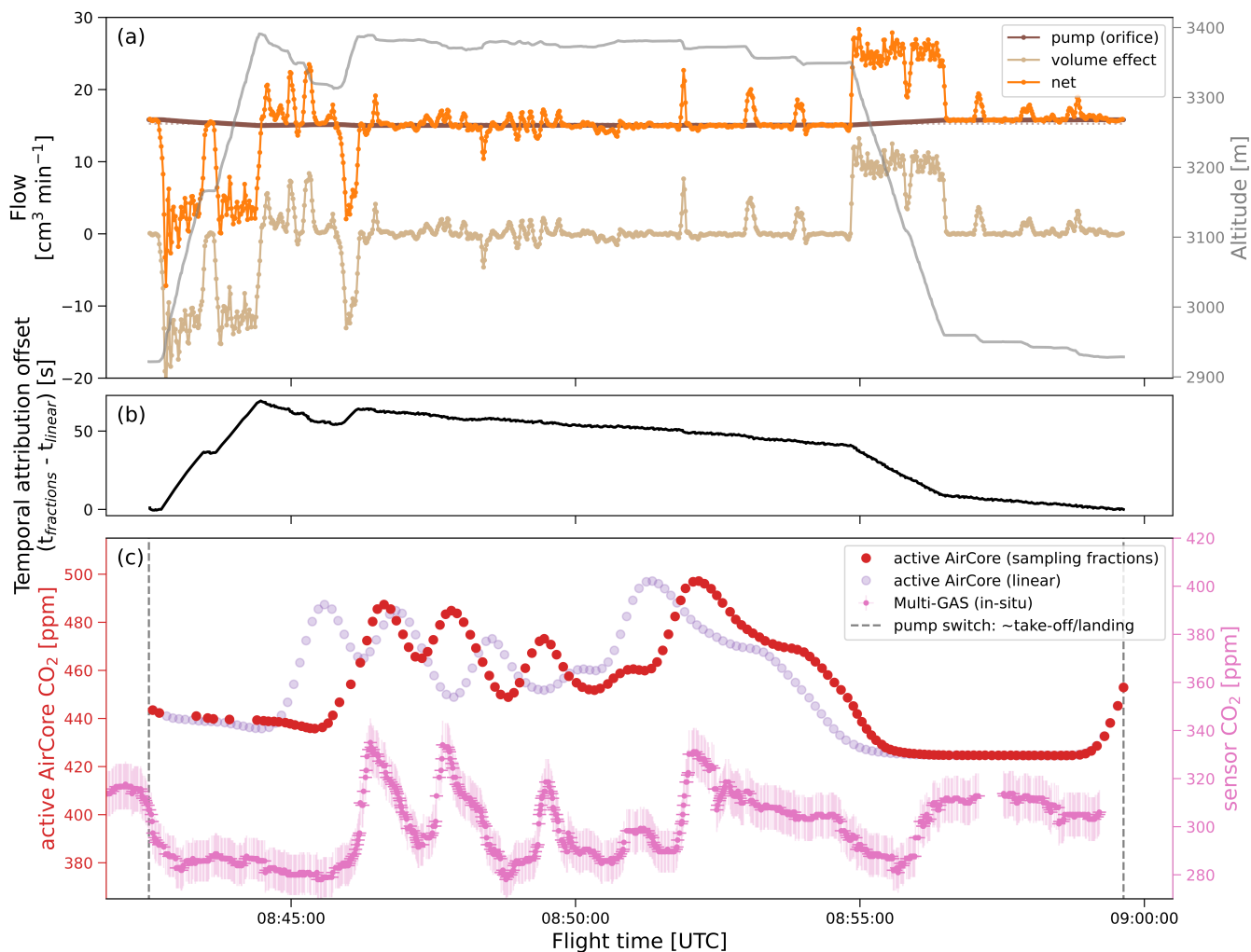


**Figure S2.** (a) Information on the sampling flow rate of the active AirCore during flight F12 (09.07.2024) alongside with (b) the temporal attribution offset corrected for by applying the proposed sampling fraction based retrieval scheme relative to the linear mapping. (c) Comparison of the active AirCore CO<sub>2</sub> measurement mapping of both retrieval approaches next to the CO<sub>2</sub> in-situ data of the Multi-GAS sensor package.

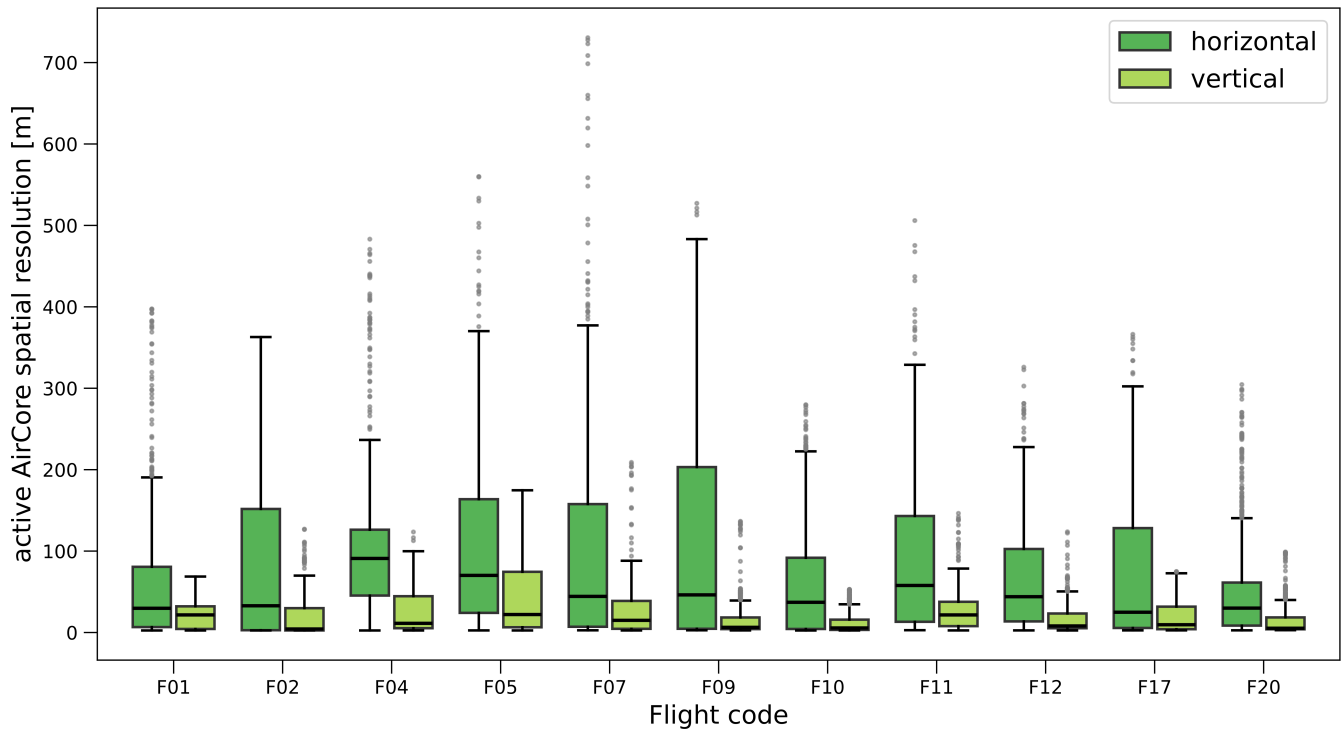


**Figure S3.** Box-Whisker-Plot showing the spatial resolution corresponding to each measurement from the active AirCore samples during the different flights. Colours indicate horizontal and vertical resolutions. The boxes extend from the first quartile to the third quartile with a line at the median. The whiskers include all data points lying within 1.5 times the interquartile range, points are outliers.

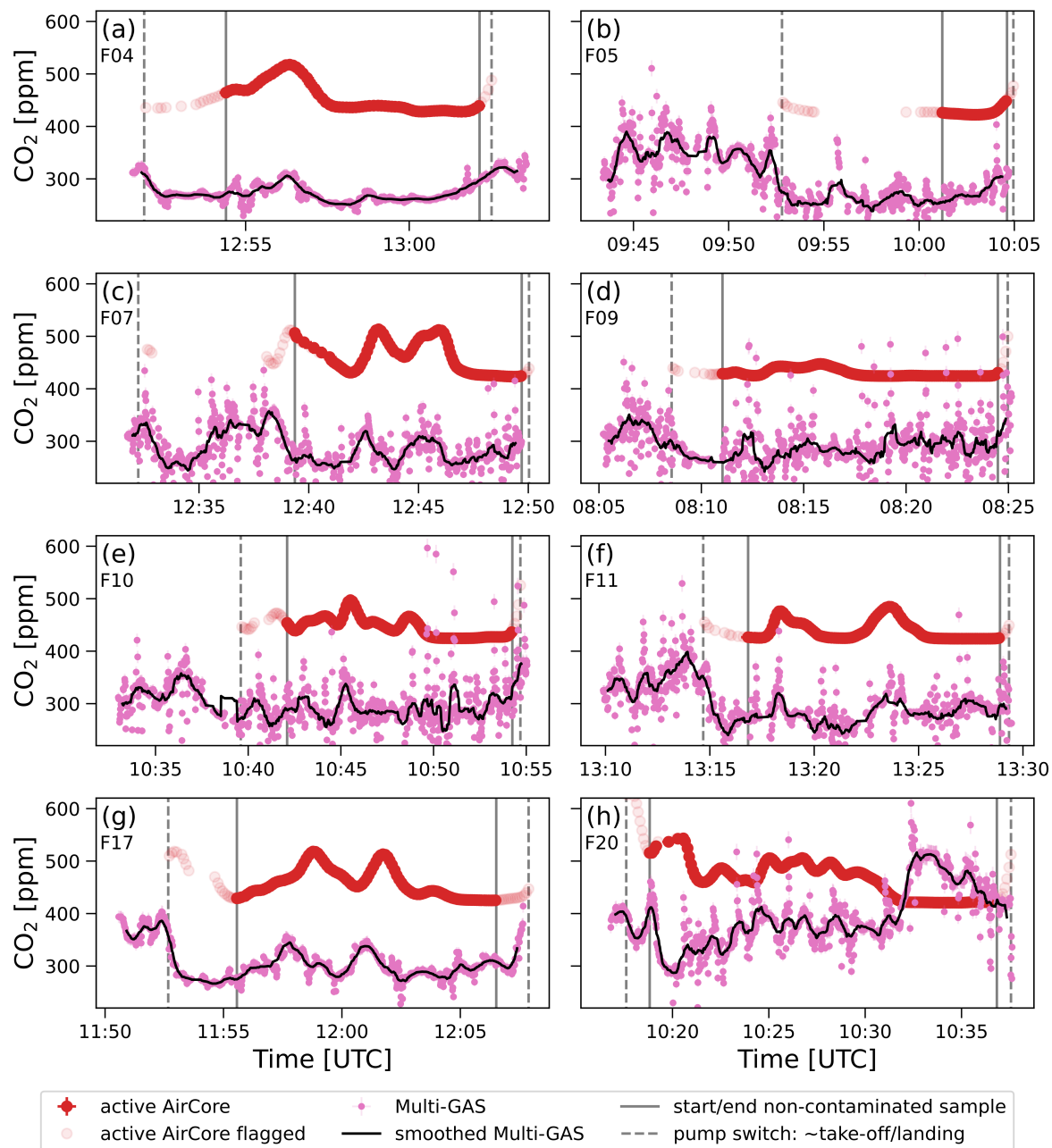


**Figure S4.** Comparison of CO<sub>2</sub> measurements from the active AirCore technique with the Multi-GAS electrochemical sensor package during the different flights (panels a-h). Note that F01 and F02 are not shown because of missing Multi-Gas data and F12 is presented in Fig. 4.

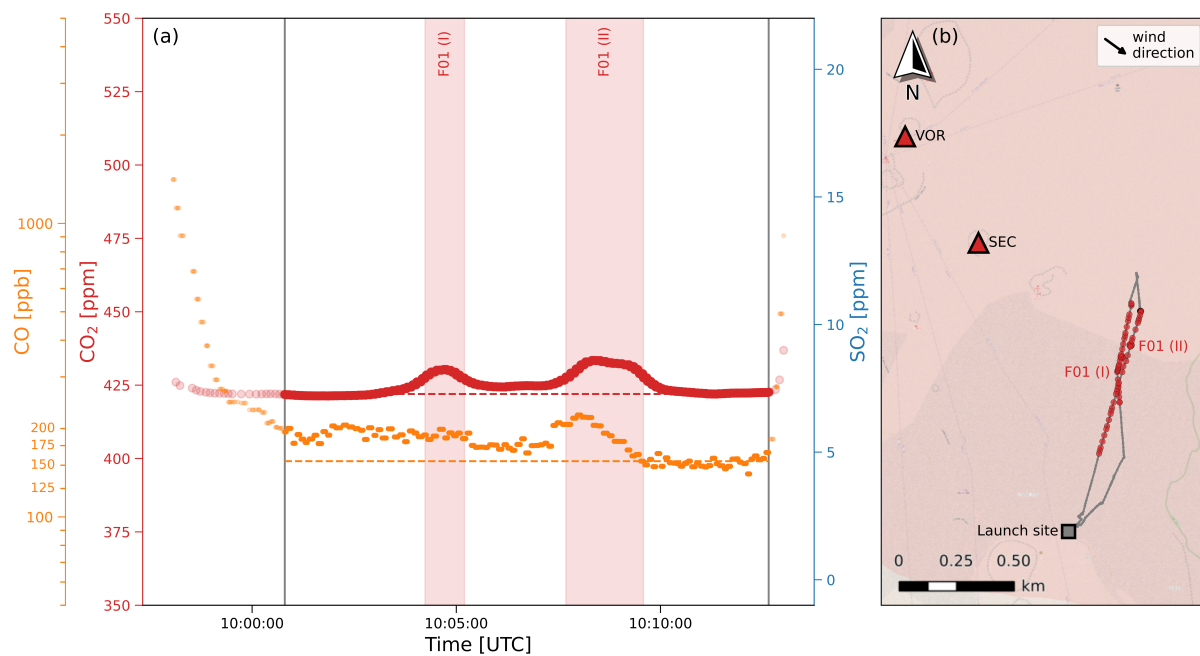


**Figure S5.** As Fig. 5 for flight F01. Note that the SO<sub>2</sub> sensor was not operated during F01.

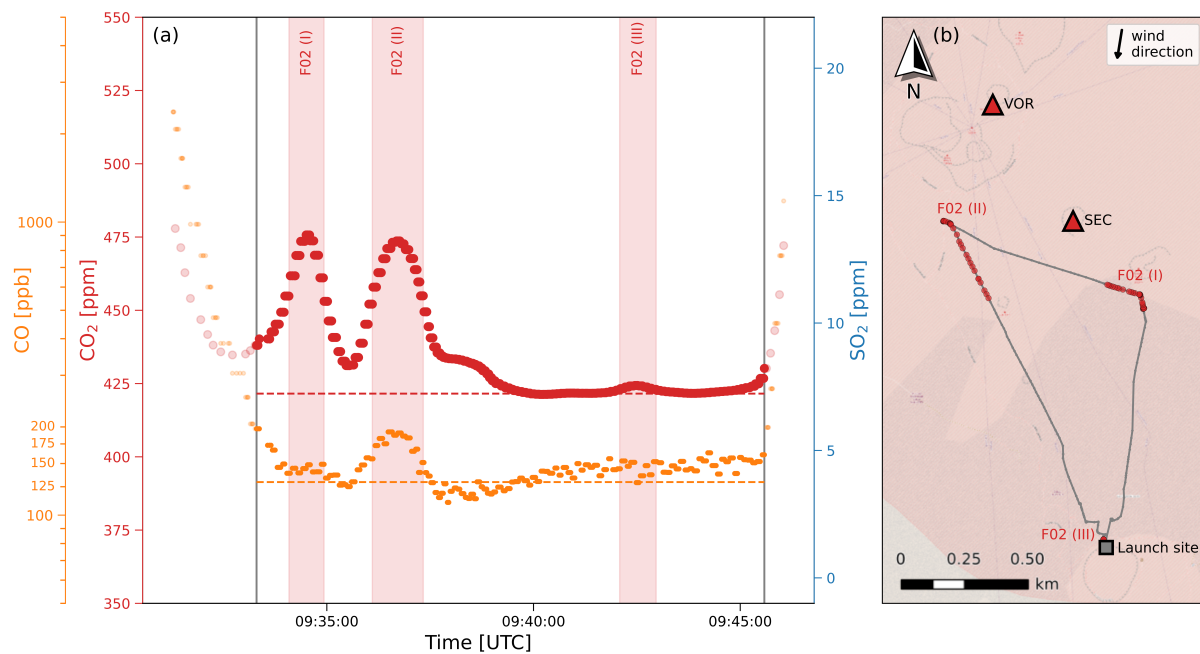


**Figure S6.** As Fig. 5 for flight F02. Note that the SO<sub>2</sub> sensor was not operated during F02.

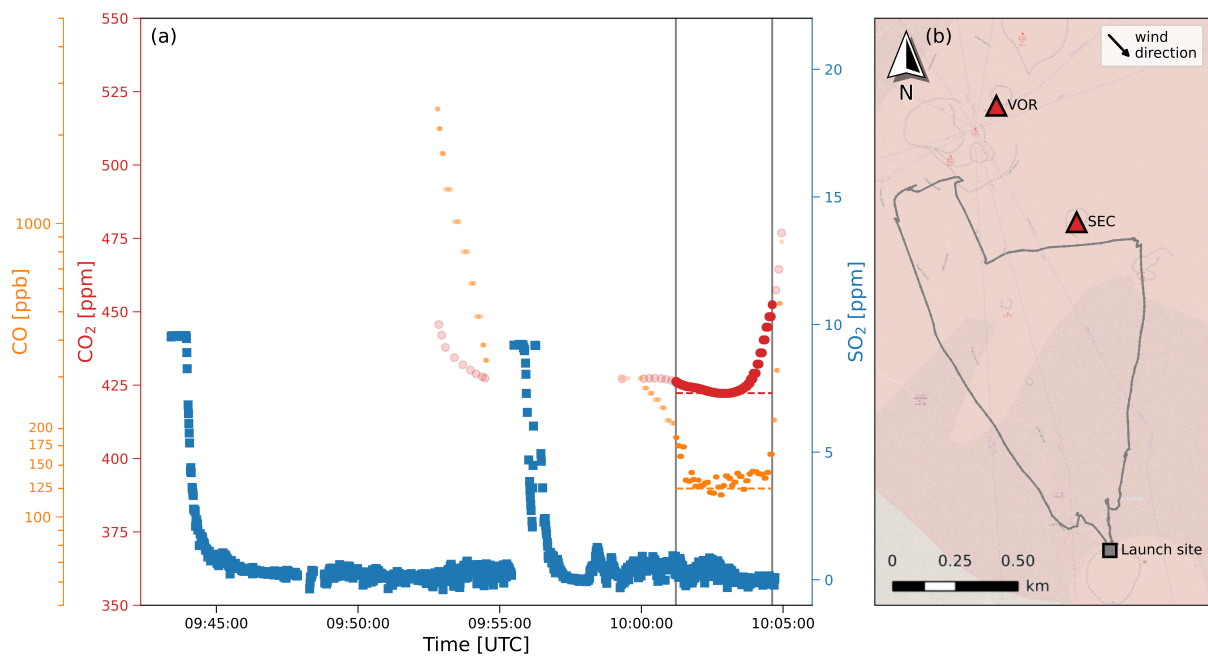


**Figure S7.** As Fig. 5 for flight F05. Note that the sampling pump did not work during parts of the flight due to a power cut.

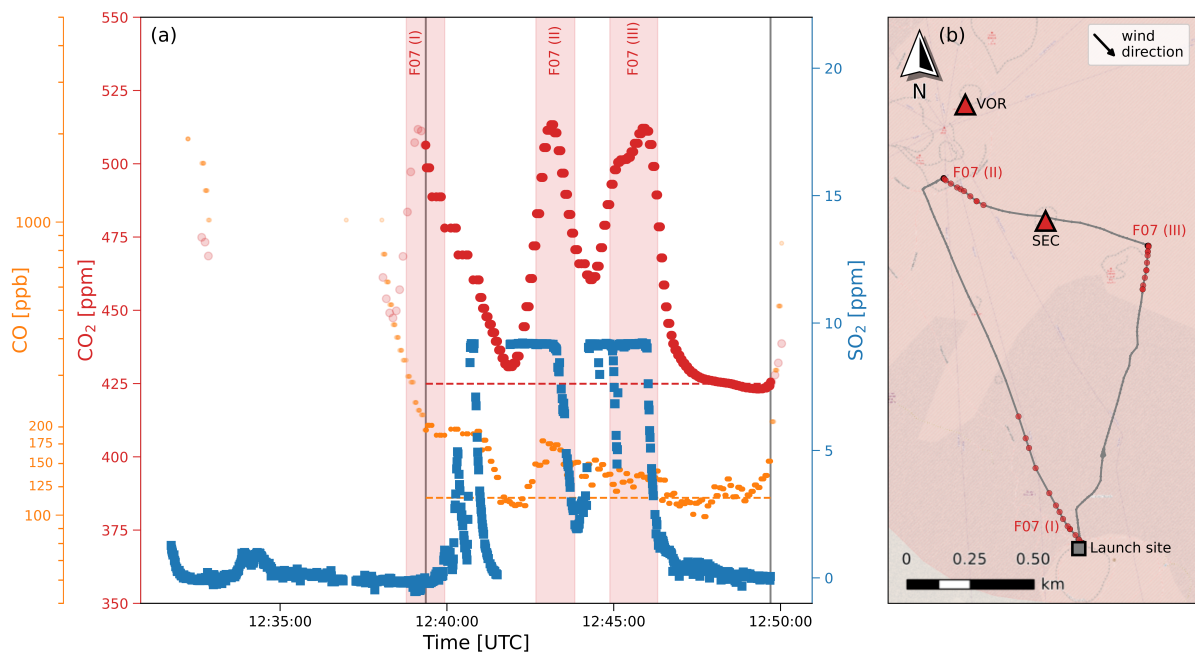


**Figure S8.** As Fig. 5 for flight F07.

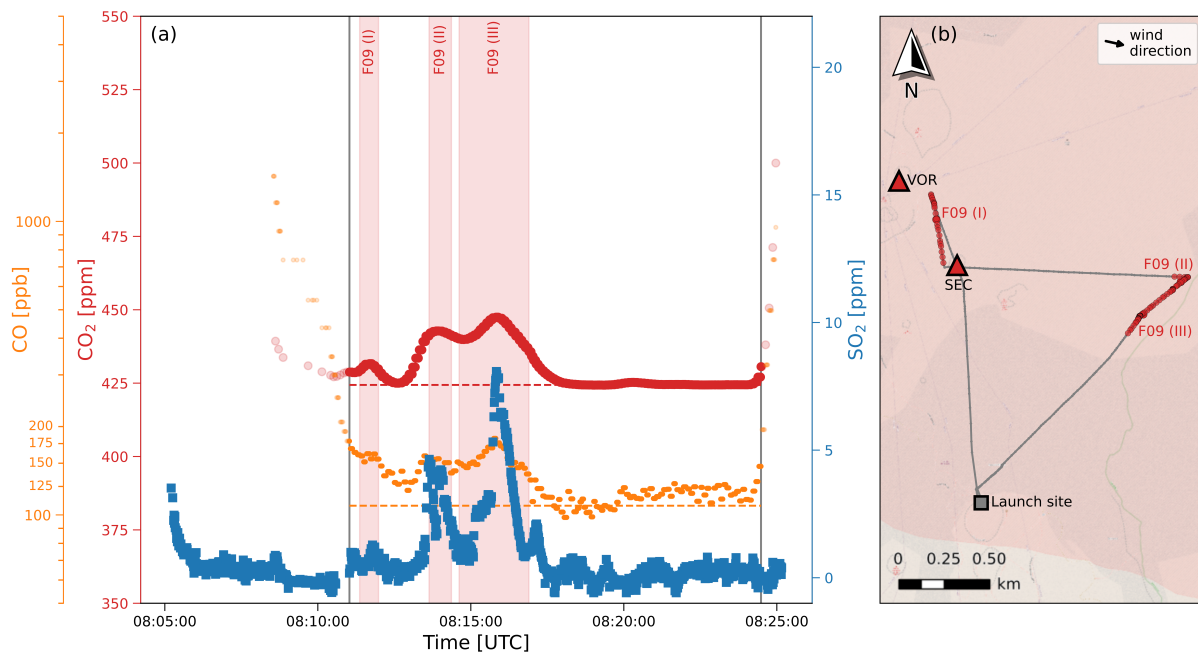


**Figure S9.** As Fig. 5 for flight F09.

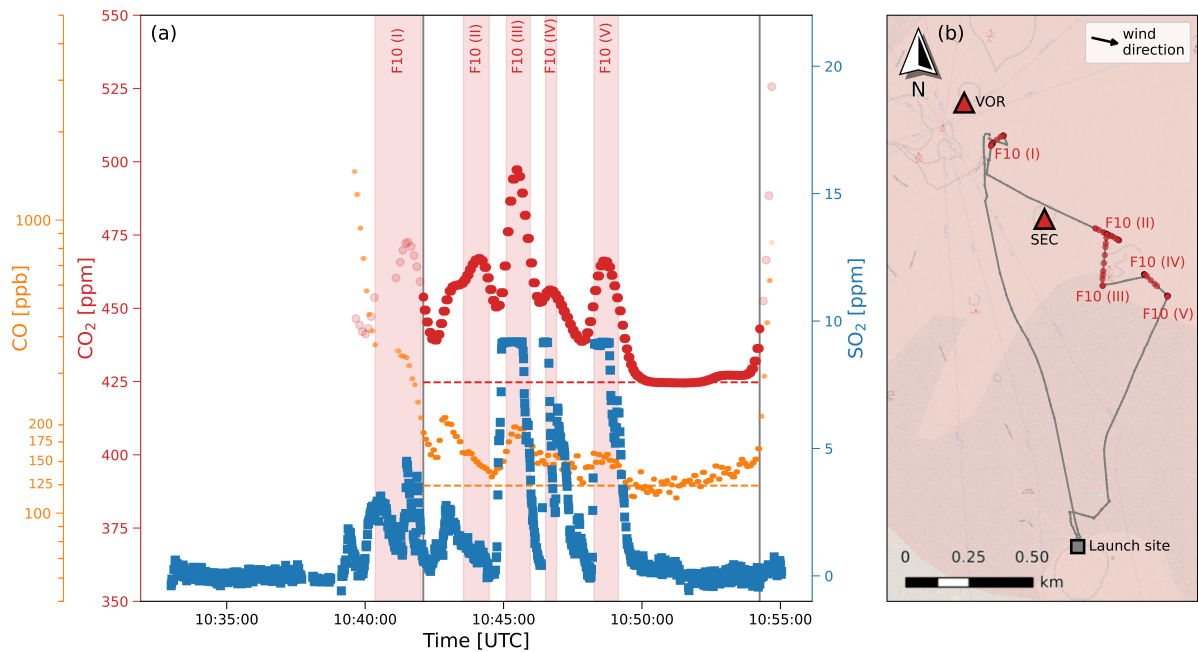


**Figure S10.** As Fig. 5 for flight F10.

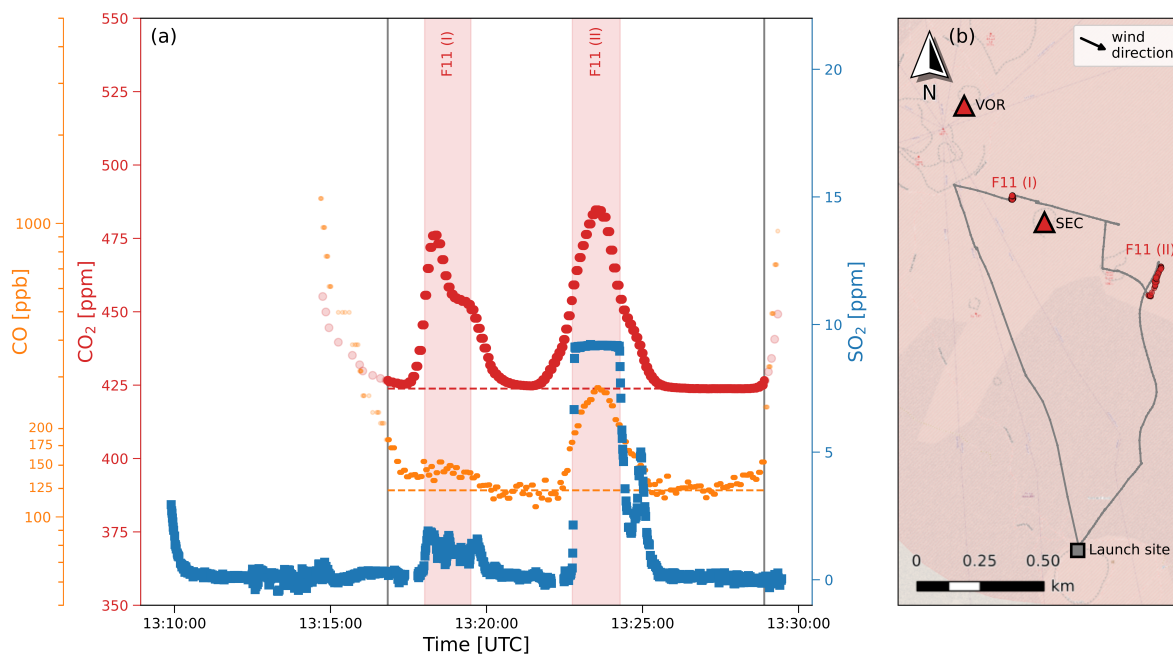


**Figure S11.** As Fig. 5 for flight F11.

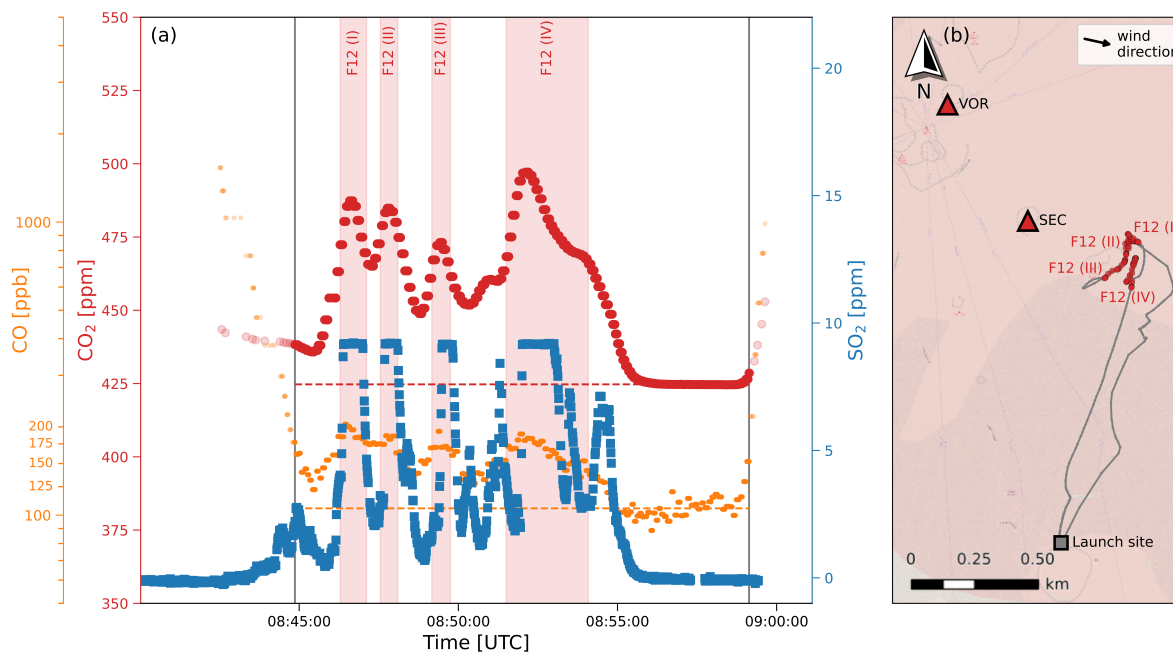


**Figure S12.** As Fig. 5 for flight F12.

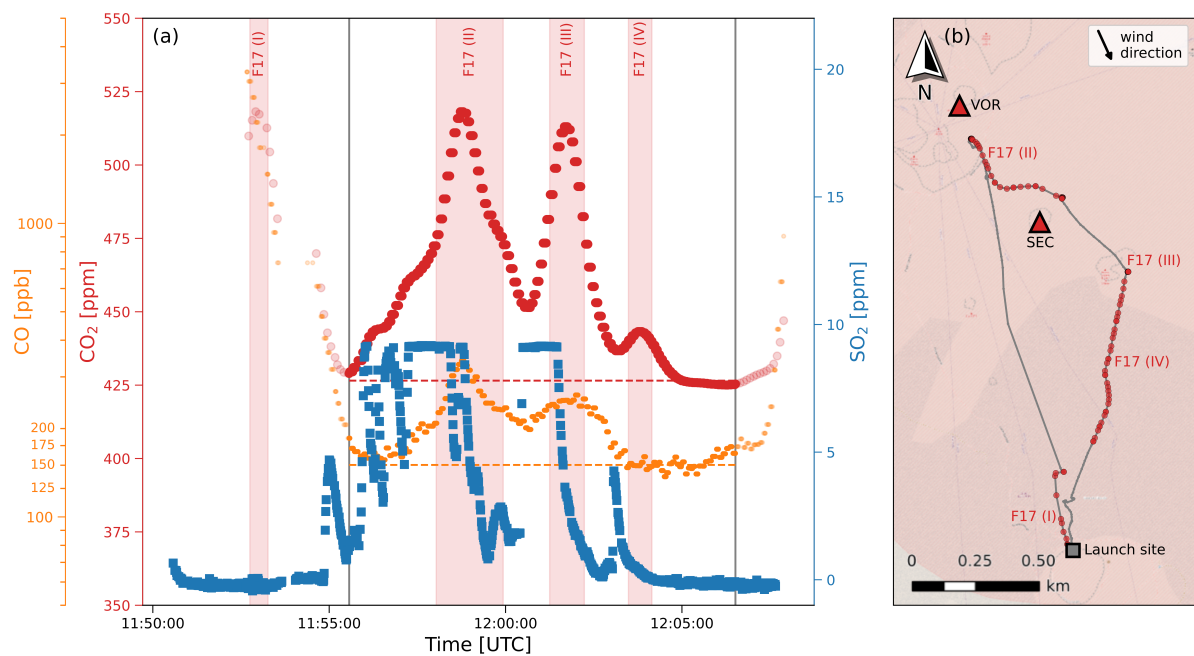


**Figure S13.** As Fig. 5 for flight F17. The post-flight analysis of this AirCore sample was done at Milo village resulting in a longer storage time and a greater altitude and resulting pressure change during storage. This causes an additional uncertainty in the matching of the AirCore sample onto the flight track. The SO<sub>2</sub> sensor signal and the CO and CO<sub>2</sub> peaks do not match as well as for the previous flights.

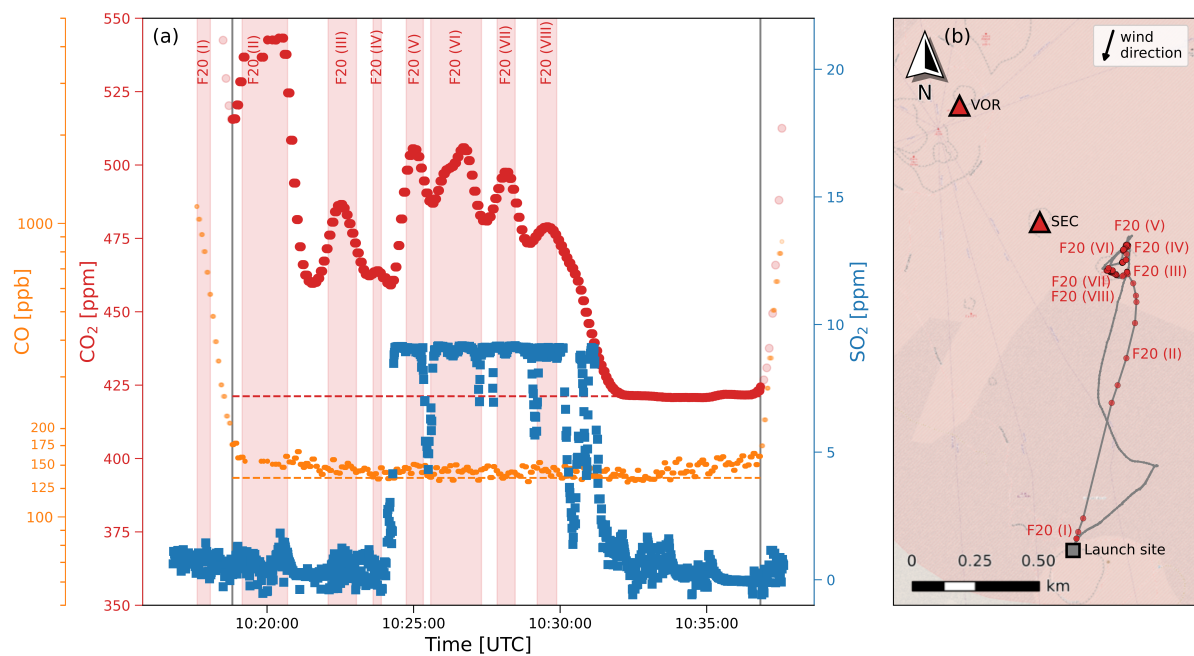


**Figure S14.** As Fig. 5v for flight F20. The post-flight analysis of this AirCore sample was done at Milo village resulting in a longer storage time and a greater altitude and resulting pressure change during storage. This causes an additional uncertainty in the matching of the AirCore sample onto the flight track. The SO<sub>2</sub> sensor signal and the CO and CO<sub>2</sub> peaks do not match as well as for the previous flights.

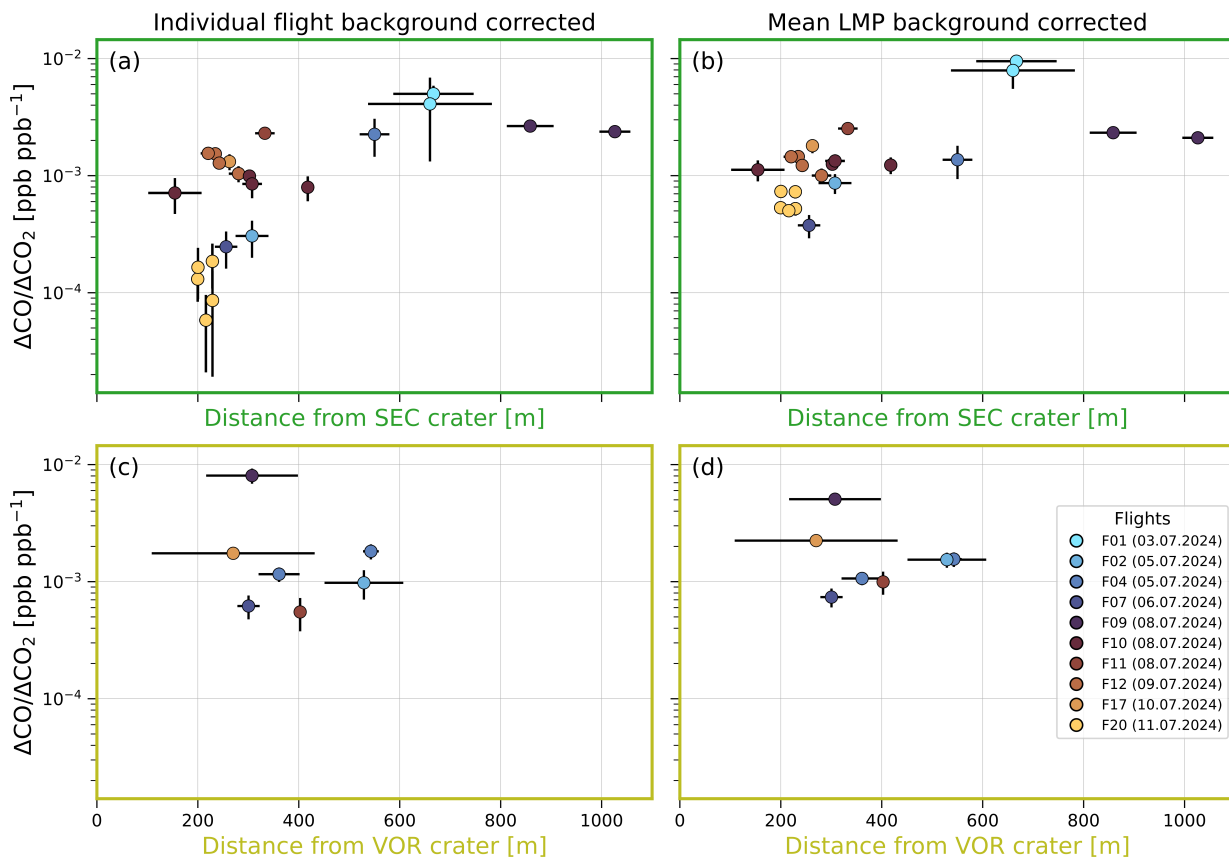


**Figure S15.** Dependency of the calculation results of the  $\Delta\text{CO}/\Delta\text{CO}_2$  ratio on distance of the sampling location from the crater, and on the choice of local or regional background criterion: The upper panels show only ratios for samples very likely influenced by South-East crater (SEC) degassing and the distance to its crater position, the lower panels the same for the Voragine crater (VOR). Panels (a) and (c) are based on the individual flight background correction scheme whereas (b) and (d) rely on the mean background values during the campaign period from Lampedusa (LMP) ICOS station.